Generalized theory of the photoacoustic effect in a multilayer material

Hanping Hu,[a) Xinwei Wang, and Xianfan Xu[b)

School of Mechanical Engineering, Purdue University, West Lafayette, Indiana 47907

In this work, a generalized expression of the photoacoustic (PA) effect in a multilayer material is derived. This expression takes thermal and optical properties and geometry of a multilayer structure, as well as the thermal contact resistances between layers into consideration. In addition, a composite piston model consisting of a thermal piston and a mechanical piston of the PA effect is developed and interpreted from the viewpoint of thermodynamics. Mistakes occurring in the thermal piston model and in the composite piston model developed before are pointed out and corrected. It is also shown that the PA effect has an isochoric character for the thermal piston and a polytropic character with a polytropic factor of $(2-1/\gamma)$ for the mechanical piston. The theory developed in this work is in good agreement with the experimental results, and is applicable to a wide range of photoacoustic problems. © *1999 American Institute of Physics.* [S0021-8979(99)05519-X]

I. INTRODUCTION

For the last two decades, the photoacoustic (PA) technique has attracted considerable attention, and has become a valuable analytical and research tool used extensively in many aspects of science and technology. The PA technique has the capability of analyzing the optical and thermal properties and geometry of multilayer materials, and nondestructive depth profiling because of critical damping of induced heat conduction. A quantitative understanding of the PA effect was first given by Rosencwaig and Gersho,[1] known as the RG model. Since then, many extensions and applications of the RG model have been developed, basically into two directions. One was to further study the basic mechanism of the PA effect. By including mechanical vibration of the sample surface, McDonald and Wetsel[2] presented a composite piston model, which was especially important for liquid due to its high thermal expansion coefficient. The other attempt was to generalize Rosencwaig and Gersho's work to multilayer samples due to the increasing importance of these materials, especially in the microelectronics industry. The majority of these studies were limited to two or three layers.[3,4] Solutions for multilayer systems[5,6] were obtained either for very special cases or under the assumption that incident light was entirely absorbed at the surface of sample. In a multilayer sample, light can be absorbed by the layers beneath the surface, even by the backing material (the substrate). Moreover, almost all these works took the thermal contact resistance between layers out of consideration. Recently, Cole and McGahan[7] developed a general solution for the temperature distribution of a multilayer system, which accounted for optical absorption in any layer as well as the contact resistances. To use their solution to calculate the temperature field, numerical integration is required.

In this article, a generalized PA model for multilayer samples is developed and the solution of the PA effect is derived in matrix expressions. No numerical integration is needed. This solution takes thermal and optical properties and geometry of a multilayer structure, as well as the thermal contact resistance between layers into consideration. Every layer, including the backing material can be light absorbing. In addition, it is pointed out that the dual-piston model of the photoacoustic effect is a result of thermodynamics principles. The physical meaning of each piston is interpreted, and the mistakes that occurred in Rosencwaig and Gersho's thermal piston model and McDonald and Wetsel's composite piston model are recognized and corrected. The theory developed in this work is verified with a number of PA measurements.

II. GENERALIZED PA SOLUTION

A typical PA apparatus is shown in Fig. 1. The heating source, usually a laser, is modulated either internally or by a mechanical chopper. The laser beam is directed onto the sample mounted at the bottom of a PA cell. The periodic change of the temperature in the gas cell causes a periodic change of pressure in gas, which can be sensed as an acoustic wave. The pressure change of the gas is also induced by the mechanical vibration at the target surface due to thermal expansion. A microphone senses the acoustic signal and transfers it to a lock-in amplifier, which measures the amplitude and phase of the acoustic signal at the modulation frequency.

In this work, the development of a generalized solution of the PA pressure signal is based on two guidelines. One is generality, the model should be applicable to as many cases as possible; the other is simplicity, the resulting expression is not too complex to use. In this session, the expression for the temperature variation in the multilayer sample and gas due to heating of the laser beam is first derived. Then the expression for the PA signal due to the temperature change and the surface expansion is developed.

[a)On leave from the Department of Thermal Science and Energy Engineering, University of Science and Technology of China, China.

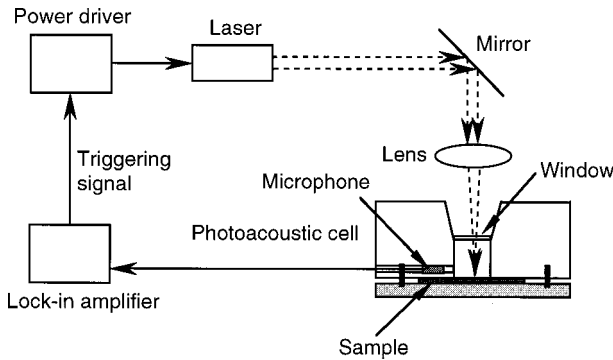[b)To whom correspondence should be addressed; electronic mail: xxu@ecn.purdue.edu

FIG. 1. Schematic of a photoacoustic apparatus.

A. Temperature distribution in multilayers

The temperature change in the gas cell is due to two effects: one is conduction heating through the contact with the sample surface, the other is mechanical work imposed on the gas medium due to vibration of the sample surface.

1. Temperature variation due to heat conduction

The cross-sectional view of a multilayer sample is shown in Fig. 2. The light source is assumed to be a sinusoidally modulated monochromatic laser beam of wavelength λ, incident through the nonabsorbing gas on the sample with flux $I = I_0(1 + \cos \omega t)/2$, where ω is the modulated angular frequency of the incident light. The sample is composed of N layers with indices 1 through N. The indices of the backing material and gas are 0 and $N+1$, which also take the subscripts b and g, respectively. Layer i, with the rear and front interface located at l_{i-1} and l_i, has a thickness of $L_i = l_i - l_{i-1}$, thermal conductivity k_i, specific heat c_{p_i}, thermal diffusivity α_i and optical absorption coefficient β_i, where $i = 0,1,..., N+1$. Some other parameters used in the derivation are the thermal diffusion length $\mu_i = \sqrt{2\alpha_i/\omega}$, thermal diffusion coefficient $a_i = 1/\mu_i$, and thermal contact resistance between layer i and $(i+1)$, $R_{i,i+1}$. Multiple reflections between interfaces and convective heat transfer in the gas cell are neglected. β_{N+1} and $R_{N,N+1}$ are taken as 0 in the gas layer. To eliminate resonance in a PA experiment, the modulation frequency ω and the typical dimension of the gas cell L_g should be selected so that $L_g < \Lambda_s/2$, where Λ_s is the minimum wavelength of the sound wave in the gas cell calculated by the maximum frequency used in the measurement.

It has been recognized that the one-dimensional heat transfer model is adequate for describing the temperature variation under typical experimental conditions when the thermal diffusion length in gas and in the target is much less
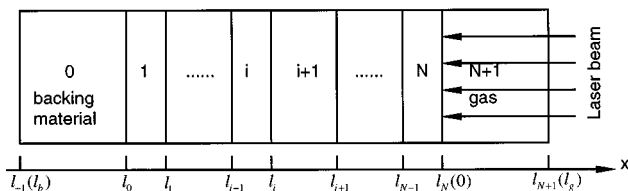

FIG. 2. Schematic of a N-layer sample.

than the diameter of laser beam. Therefore, the thermal diffusion equation in layer i can then be expressed as

$$\frac{\partial^2 \theta_i}{\partial x^2} = \frac{1}{\alpha_i}\frac{\partial \theta_i}{\partial t} - \frac{\beta_i I_0}{2k_i}\exp\left(\sum_{m=i+1}^{N} -\beta_m L_m\right)$$
$$\times e^{\beta_i(x-l_i)}(1 + e^{j\omega t}), \tag{1}$$

where $\theta_i = T_i - T_{amb}$ is the modified temperature in layer i, and T_{amb} is the ambient temperature. The solution θ_i of the above thermal diffusion equation set consists of three parts: the transient component $\theta_{i,t}$, the steady dc component $\bar{\theta}_{i,s}$, and the steady ac component $\tilde{\theta}_{i,s}$. Therefore,

$$\theta_i = \theta_{i,t} + \bar{\theta}_{i,s} + \tilde{\theta}_{i,s}. \tag{2}$$

Because in a PA measurement, the lock-in amplifier only picks up the ac components, only $\tilde{\theta}_{i,s}$ needs to be evaluated here. $\tilde{\theta}_{i,s}$ is resulted from the periodic source term $-(\beta_i I_0/2k_i)\exp(\Sigma_{m=i+1}^{N} - \beta_m L_m)e^{\beta_i(x-l_i)}e^{j\omega t}$ in Eq. (1). When this source term is considered, Eq. (1) has a particular solution in the form of $-E_i e^{\beta_i(x-l_i)}e^{j\omega t}$, where $E_i = G_i/(\beta_i^2 - \sigma_i^2)$ with $G_i = (\beta_i I_0/2k_i)\exp(-\Sigma_{m=i+1}^{N}\beta_m L_m)$ for $i < N$, $G_N = \beta_N I_0/2k_N$, and $G_{N+1} = 0$. σ_i is defined as $(1+j)a_i$ with $j = \sqrt{-1}$. The general solution of $\tilde{\theta}_{i,s}$ can be expressed in the form of

$$\tilde{\theta}_{i,s} = [A_i e^{\sigma_i(x-h_i)} + B_i e^{-\sigma_i(x-h_i)} - E_i e^{\beta_i(x-h_i)}]e^{j\omega t}, \tag{3}$$

where A_i and B_i are the coefficients to be determined, and h_i is calculated as $h_i = l_i$ for $i = 0,1,...,N$, and $h_{N+1} = 0$.

In most PA experiments, the modulation frequency is greater than 100 Hz, thus the thermal diffusion length in gas and in the backing material is less than 0.3 mm. It is therefore reasonable to assume that the gas and the backing layer are thermally thick, meaning $|\sigma_0 L_0| \gg 1$ and $|\sigma_{N+1}L_{N+1}| \gg 1$. Based on this assumption, the coefficients A_{N+1} and B_0 can be taken as zero. The rest of the coefficients A_i and B_i can be determined by using the interfacial conditions at $x = l_i$

$$k_i\frac{\partial \tilde{\theta}_{i,s}}{\partial x} - k_{i+1}\frac{\partial \tilde{\theta}_{i+1,s}}{\partial x} = 0, \tag{4a}$$

$$k_i\frac{\partial \tilde{\theta}_{i,s}}{\partial x} + \frac{1}{R_{i,i+1}}(\tilde{\theta}_{i,s} - \tilde{\theta}_{i+1,s}) = 0. \tag{4b}$$

Equations (4a) and (4b) indicate that the heat flux at the interfaces between layers is continuous, while the temperatures are not when thermal contact resistances exist. From Eqs. (4a) and (4b), the recurrence formula of the coefficients A_i and B_i of Eq. (3) is obtained in a matrix form as

$$\begin{bmatrix} A_i \\ B_i \end{bmatrix} = U_i\begin{bmatrix} A_{i+1} \\ B_{i+1} \end{bmatrix} + V_i\begin{bmatrix} E_i \\ E_{i+1} \end{bmatrix}, \tag{5}$$

where

$$U_i = \frac{1}{2}\begin{bmatrix} u_{11,i} & u_{12,i} \\ u_{21,i} & u_{22,i} \end{bmatrix}; V_i = \frac{1}{2}\begin{bmatrix} v_{11,i} & v_{12,i} \\ v_{21,i} & v_{22,i} \end{bmatrix}, \tag{6a}$$

$$u_{1n,i} = (1 \pm k_{i+1}\sigma_{i+1}/k_i\sigma_i \mp k_{i+1}\sigma_{i+1}R_{i,i+1})$$
$$\times \exp[\mp \sigma_{i+1}(h_{i+1} - h_i)], \quad n = 1,2, \tag{6b}$$

$$u_{2n,i} = (1 \mp k_{i+1}\sigma_{i+1}/k_i\sigma_i \mp k_{i+1}\sigma_{i+1}R_{i,i+1})$$
$$\times \exp[\mp \sigma_{i+1}(h_{i+1}-h_i)], \quad n=1,2, \quad (6c)$$

$$v_{n1,i} = 1 \pm \beta_i/\sigma_i, n=1,2, \quad (6d)$$

$$v_{n2,i} = (-1 \mp k_{i+1}\beta_{i+1}/k_i\sigma_i + k_{i+1}\beta_{i+1}R_{i,i+1})$$
$$\times \exp[-\beta_{i+1}(h_{i+1}-h_i)]. \quad (6e)$$

The physical interpretation of U_i is the interfacial transmission matrix of heat from layer $(i+1)$ to i,[8] and V_i is the absorption matrix of light.

Based on Eqs. (5)–(6e), along with $A_{N+1}=0$ and $B_0=0$, after some recurrent operations, the coefficients A_i and B_i are obtained as

$$B_{N+1} = - \frac{[0 \quad 1]\Sigma_{m=0}^N(\Pi_{i=0}^{m-1}U_i)V_m\begin{bmatrix} E_m \\ E_{m+1} \end{bmatrix}}{[0 \quad 1](\Pi_{i=0}^N U_i)\begin{bmatrix} 0 \\ 1 \end{bmatrix}}; \quad (7a)$$

$$\begin{bmatrix} A_i \\ B_i \end{bmatrix} = \left(\Pi_{m=i}^N U_m\right)\begin{bmatrix} 0 \\ B_{N+1} \end{bmatrix}$$
$$+ \sum_{m=i}^N \left(\Pi_{k=i}^{m-1}U_k\right)V_m\begin{bmatrix} E_m \\ E_{m+1} \end{bmatrix}, \quad (7b)$$

where $\Pi_{k=i}^{i-1}U_k$ is taken as $\begin{bmatrix} 1 & 0 \\ 0 & 1 \end{bmatrix}$.

Substituting Eq. (7) into Eq. (3), the ac temperature distribution $\tilde{\theta}_{i,s}$ in layer i can be obtained. In particular, the ac temperature distribution in the gas can be found as:

$$\tilde{\theta}_{N+1,s} = B_{N+1}e^{-\sigma_{N+1}x}e^{j\omega t}. \quad (8)$$

2. Temperature variation due to surface vibration

When the sample is heated by modulated laser light, the thermal expansion of the sample causes mechanical vibration at its surface, which imposes work on the gas, causing an additional temperature change $\delta\tilde{\theta}_{i,s}$. Computation of this additional temperature change is described below.

The work done by the surface vibration on the gas is $p_{amb}\Delta x_s S$, where p_{amb} is the ambient pressure, S is the area of the sample surface irradiated by the laser beam and Δx_s is the displacement of sample surface due to the thermal expansion of sample, expressed as $\Delta x_0 e^{j\omega t+\theta_{lag}}$, where Δx_0 and θ_{lag} are the amplitude and the phase shift of vibration, respectively. The thermal diffusion equation in layer i can be expressed as

$$\frac{\partial^2(\delta\tilde{\theta}_{i,s})}{\partial x^2} = \frac{1}{\alpha_i}\frac{\partial(\delta\tilde{\theta}_{i,s})}{\partial t} - \frac{j\omega p_{amb}\Delta x_0}{L_g k_{N+1}}e^{j(\omega t+\theta_{lag})}$$
$$(l_N < x < l_{N+1}) \text{ for } i=N+1, \quad (9a)$$

$$\frac{\partial^2(\delta\tilde{\theta}_{i,s})}{\partial x^2} = \frac{1}{\alpha_i}\frac{\partial(\delta\tilde{\theta}_{i,s})}{\partial t}$$
$$(l_{i-1} < x < l_i) \text{ for } i=0,1,2,....N. \quad (9b)$$

The interfacial conditions at $x=l_i$ are the same as Eqs. (4a) and (4b). Since only the temperature variation in the gas is of interest, using the similar derivation procedure as above, it is calculated as

$$\delta\tilde{\theta}_{N+1,s} = -\left(\frac{[0 \quad 1](\Pi_{i=0}^{N-1}U_i)\begin{bmatrix} 1 \\ 1 \end{bmatrix}}{[0 \quad 1](\Pi_{i=0}^N U_i)\begin{bmatrix} 0 \\ 1 \end{bmatrix}}e^{-\sigma_{N+1}x} - 1\right)$$
$$\times \frac{\alpha_{N+1}p_{amb}\Delta x_0}{L_g k_{N+1}}e^{j(\omega t+\theta_{lag})}. \quad (10)$$

B. Photoacoustic signal

The photoacoustic signal is due to the acoustic wave in the gas cell induced by the incident light on the sample. To investigate the inherent mechanisms of the PA effect, the thermoacoustic response of the gas needs to be studied. According to the basic principle of thermodynamics, there are relations among intensive thermodynamic properties, namely the equations of state. For any substance, it is possible to specify an intensive thermodynamic property by any other two intensive thermodynamic properties. Thus, for the gas in the PA cell, in terms of its pressure p, temperature T and volume V, the equation of state can be written as $p=p(T,V)$, from which the total differential pressure of gas can be represented as

$$dp = \left(\frac{\partial p}{\partial T}\right)_V dT + \left(\frac{\partial p}{\partial V}\right)_T dV. \quad (11)$$

Assuming the gas is ideal, then

$$\left(\frac{\partial p}{\partial T}\right)_V = \frac{p}{T}, \left(\frac{\partial p}{\partial V}\right)_T = -\frac{p}{V}. \quad (12)$$

Since the design of PA cell requires $L_g < \Lambda_s/2$, p is uniform in the entire domain of the gas cell. However, there is a temperature distribution in the gas arising from radiation of incident light on the surface of the sample. For this reason, along with considering Eq. (12), Eq. (11) can be rearranged as

$$dp = \frac{p}{T}\langle dT\rangle - \frac{p}{V}dV, \quad (13)$$

where $\langle dT\rangle$ is the volume average of temperature variation of the gas in the cell. Physically, dp produces the acoustic signal. $dT=\tilde{\theta}_{N+1,s}+\delta\tilde{\theta}_{N+1,s}$, $dV=-\Delta V_s$, with ΔV_s, the volumetric thermal expansion of the sample, $p=p_{amb}$, $T=T_{amb}$, and $V=V_g$, the total volume of the gas cell. Therefore, Eq. (13) can be rewritten as

$$dp = \frac{p_{amb}}{T_{amb}}\langle\tilde{\theta}_{N+1,s}\rangle + \left[\frac{p_{amb}}{V_g}\Delta V_s + \frac{p_{amb}}{T_{amb}}\langle\delta\tilde{\theta}_{N+1,s}\rangle\right]. \quad (14)$$

Although no piston concept is employed in the above derivation, Eq. (14) gives the expression of the composite-piston model, but is derived from the view point of thermodynamics. The first term on the right-hand side of Eq. (14) represents the thermal piston effect resulting from the thermal expansion of gas heated by the sample, which only occurs in

TABLE I. PA signal from a carbon-black sample in a gas cell filled with Ar, N_2, or $CCIF_3$.

i	γ_i	S_i (mV) [experiment (Ref. 10)]	S_{Ar}/S_i [experiment (Ref. 10)]	S_{Ar}/S_i (RG model)	S_{Ar}/S_i (the current model)
Ar	1.67	7.8 ± 0.2	1	1	1
N_2	1.40	7.9	0.99	1.15	0.96
$CCIF_3$	1.17	3.5 ± 0.1	2.23	3.16	2.21

a narrow layer in the gas adjacent to the sample and pushes the rest of gas just like a piston. The term in the bracket can be interpreted as a result of the mechanical piston effect due to the thermal expansion of the sample.

The pressure variation caused by the thermal piston, dp_t, is calculated by averaging the temperature change in the gas as

$$dp_t = \frac{p_{amb}}{T_{amb}} \langle \tilde{\theta}_{N+1,s} \rangle = \frac{p_{amb}}{T_{amb}L_g} \int_0^{L_g} B_{N+1} e^{-\sigma_{N+1}x} dx e^{j\omega t}$$

$$= \frac{p_{amb}B_{N+1}}{\sqrt{2}T_{amb}L_g a_g} e^{j(\omega t - \pi/4)}. \quad (15)$$

Compared with the result by Rosencwaig and Gersho,[1] $dp_t = (\gamma p_{amb}B_{N+1}/\sqrt{2}T_{amb}L_g a_g)e^{j(\omega t - \pi/4)}$, Eq. (15) does not include $\gamma(=c_p/c_v)$.

The pressure variation caused by the mechanical piston, dp_m, is calculated as

$$dp_m = \frac{p_{amb}}{V_g} \Delta V_s + \frac{p_{amb}}{T_{amb}} \langle \delta\tilde{\theta}_{N+1,s} \rangle$$

$$= \frac{p_{amb}}{L_g} \Delta x_s + \frac{p_{amb}}{T_{amb}} \langle \delta\tilde{\theta}_{N+1,s} \rangle. \quad (16)$$

Substituting Eq. (10) into Eq. (16), dp_m can be calculated as

$$dp_m = \frac{\tilde{n}p_{amb}}{L_g} \Delta x_s, \quad (17)$$

where

$$\tilde{n} = 1 - \left(\frac{[0 \ \ 1](\Pi_{i=0}^{N-1}U_i)\begin{bmatrix}1\\1\end{bmatrix}}{[0 \ \ 1](\Pi_{i=0}^{N}U_i)\begin{bmatrix}0\\1\end{bmatrix}} \frac{e^{-(\pi/4)j}}{\sqrt{2}L_g a_g} - 1 \right) \frac{\alpha_{N+1}p_{amb}}{T_{amb}k_{N+1}}. \quad (18)$$

Considering $k_{N+1}\sigma_{N+1} \ll k_N\sigma_N$ and $L_g a_g \gg 1$, and substituting Eq. (6) into Eq. (18), the expression for $\tilde{n}$ can be simplified as $\tilde{n} = 2 - 1/\gamma$. Therefore, Eq. (17) can be rewritten as

$$dp_m = \left(2 - \frac{1}{\gamma} \right) \frac{p_{amb}}{L_g} \Delta x_s. \quad (19)$$

The result by McDonald and Wetsel[2] and McDonald,[9] $dp_m = (\gamma p_{amb}/L_g)\Delta x_s$, is different from Eq. (19) since $1 < \tilde{n} < \gamma$. The reason for the difference between Eq. (15) and Rosencwaig and Gersho's[1] model, and the difference between Eq. (19) and McDonald's[2] model lies in the assumption of the gas compressing process. In the previous models, both the thermal and mechanical compressing processes in

the gas cell are assumed to be adiabatic, however, the process is isochoric for the thermal piston and polytropic for the mechanical piston as shown in this work.

In most PA measurements, only the phase shift or the ratio of amplitudes of two samples obtained in the same gas medium are used to determine the unknown properties. Therefore, different models actually provide the same results. The only experimental data that can be used to determine the compression process in the gas cell were given by Korpiun and Büchner,[10] who used Ar, N_2, and $CCIF_3$ as the gas medium, each with a different γ value, and measured the amplitude of the PA signal S_i on carbon. The results of their measured amplitude of the PA signal, in millivolts, are listed in Table I. The ratios of the amplitudes using different gases, S_{Ar}/S_i, are calculated from the experimental data by Korpiun and Büchner, by the RG model, and by Eq. (15). Only Eq. (15) is used since for the solid sample, the PA signal due to the thermal piston is much larger than that of the mechanical piston (see below). It is seen from Table I that the RG model is different from the experimental results by a factor of γ_i/γ_{Ar}. On the other hand, the signal ratio calculated using Eq. (15) agrees well with the experimental results. Therefore, the data by Korpiun and Büchner confirmed the isochoric character of the thermal piston; the PA signal does not depend on γ.

The calculation of Δx_s in the expression of dp_m, Eq. (19), is related to the mechanical boundary conditions, and shear and bulk moduli of multilayer materials. The detailed derivation involves dealing with a set of elastic wave equations, which is more complicated than that of the temperature distribution calculation. Fortunately, for solid samples, thermal expansion is small enough to be neglected compared with that of gas, which is shown as the follows. The influence of the mechanical piston can be estimated as

$$|dp_m| = \left| \frac{\tilde{n}p_{amb}}{L_g} \Delta x_s \right| \le \left| \frac{\tilde{n}p_{amb}}{L_g} \sum_{i=0}^{N} \int_{l_{i-1}}^{l_i} \beta_{T,i}\tilde{\theta}_{i,s}dx \right|, \quad (20)$$

where $\beta_{T,i}$ is the volumetric thermal expansion coefficient of layer i. Therefore,

$$\left| \frac{dp_m}{dp_t} \right| \le \left| \frac{\tilde{n}\sqrt{2}T_{amb}a_g}{B_{N+1}} \sum_{i=0}^{N} \int_{l_{i-1}}^{l_i} \beta_{T,i}\tilde{\theta}_{i,s}dx \right|. \quad (21)$$

Using Eq. (21), for most solid samples at modulation frequencies lower than 20 kHz, $|dp_m/dp_t|$ can be estimated to be less than 1%, and the phase shift caused by the mechanical piston is less than 0.1°. Thus for solid materials, the mechanical piston effect can be neglected, and the total pressure variation is only related to the thermal piston effect as
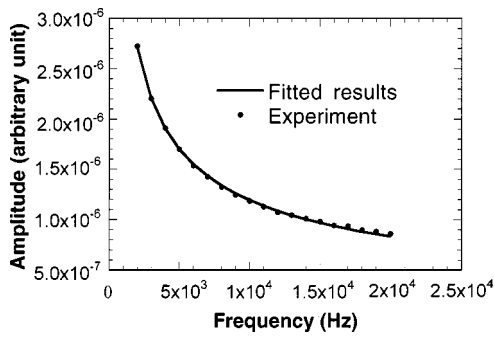
FIG. 3. Amplitude as a function of the modulation frequency for 1-mm-thick glass coated with 70-nm-thick Ni.

FIG. 5. Amplitude as a function of the modulation frequency for the Ni/SiO$_2$/Si sample.

$$dp = \frac{p_{\text{amb}}B_{N+1}}{\sqrt{2}T_{\text{amb}}L_g a_g} e^{j(\omega t - \pi/4)}. \qquad (22)$$

According to Eq. (22), the phase shift of the PA signal is calculated as $\text{Arg}(B_{N+1}) - \pi/4$, and the amplitude is calculated as $|p_{\text{amb}}B_{N+1}/\sqrt{2}T_{\text{amb}}L_g a_g|$. Considering surface reflectivity ρ, the amplitude of the pressure variation should be computed as $|(1-\rho)p_{\text{amb}}B_{N+1}/\sqrt{2}T_{\text{amb}}L_g a_g|$.

The mechanical piston could have significant contribution to the photoacoustic signal for a liquid sample. In this case, dp_m can be calculated using the following formula:

$$dp_m = \frac{\tilde{n}p_{\text{amb}}}{L_g} \sum_{i=0}^{N} \int_{l_{i-1}}^{l_i} \beta_{T,i} \tilde{\theta}_{i,s} dx. \qquad (23)$$

III. EXPERIMENTAL RESULTS AND DISCUSSIONS

The formulas derived above can be used to determine the thermal properties and geometry of either the front or buried layers, and thermal contact resistance between layers by fitting the experimental PA signals. When the surface is absorbing, these formulas can also be used to determine the optical properties. Based on the equations derived in this work, a computer code is developed to calculate the PA responses, and the least-square method is used to fit the experimental results and find the unknown properties. In order to evaluate the theoretical model developed in Sec. II, photoacoustic signals are measured as a function of the modulation frequency for a number of samples, and the data are fitted to obtain their thermal properties.
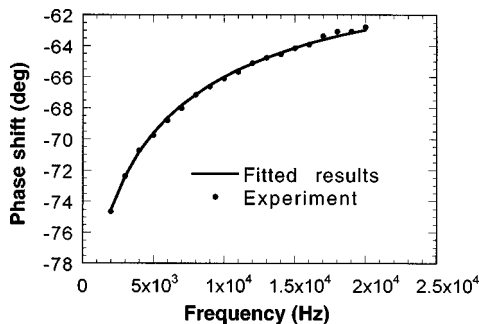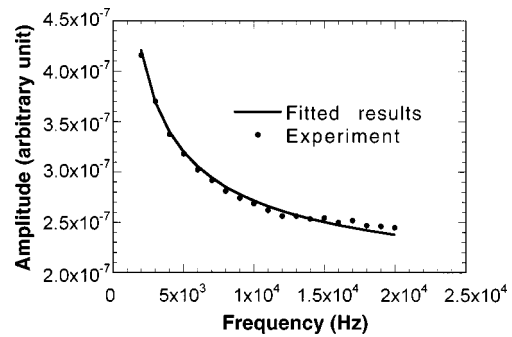
The first sample is a 1-mm-thick glass slide coated with a 70-nm-thick nickel film. By fitting the amplitude of the PA signal, the thermal conductivity of glass is found to be $1.38^{+0.05}_{-0.07}$ W/m K, close to the literature value of 1.4 W/m K.[11] The uncertainties in the thermal conductivity value is determined using numerical computation, by varying the experimental data in their uncertainty range. Results of fitting are shown in Fig. 3. It is seen that the measured amplitude of the PA signal can be well fitted with the results calculated from the theory. The relative mean-square deviation is only 1.5%.

The thermal conductivity of a 484.5-nm-thick thermally grown SiO$_2$ film on a Si substrate is measured by fitting the phase shift and the amplitude of the PA signal. The thermal conductivity of the SiO$_2$ layer is found to be 1.52 ± 0.08 W/m K by fitting the phase shift data and 1.44 ± 0.1 W/m K by fitting the amplitude data. These results are close to the thermal conductivity data of thermally grown SiO$_2$ films obtained by Okuda and Ohkubo,[12] which is 1.55 W/m K. Results of fitting are shown in Figs. 4 and 5, with a mean-square deviation of 0.38° for the phase shift data and a 1.5% relative deviation for the amplitude data.

For the two samples mentioned above, thermal contact resistances are also treated as variable parameters. It was found that the thermal conductivity and the contact resistance influence the computational results independently; no multiple solutions exist. Other parameters, such as the thickness of the samples are fixed in the calculation since they were accurately measured using other techniques. The thermal contact resistances in these two samples are found to be

FIG. 4. Phase shift as a function of the modulation frequency for the Ni/SiO$_2$/Si sample.

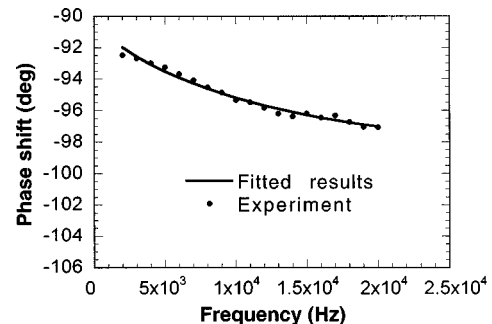FIG. 6. Phase shift as a function of the modulation frequency for 1.03-μm-thick Ni film coated on glass.

negligible (less than $10^{-9}\,\mathrm{m^2\,K/W}$). Another sample used in an e-beam evaporated 1.03-μm-thick Ni film on a 1-mm-thick glass slide. For this sample, the thermal conductivity of the Ni film and the thermal contact resistance between the Ni film and the glass slide are treated as two variable parameters. Using phase shift fitting, the thermal conductivity of is found to be $1.17\pm0.08\,\mathrm{W/m\,K}$, and the thermal contact resistance is found to be $5.30\pm1.8\times10^{-7}\,\mathrm{m^2\,K/W}$. Validation of these two values with literature data is not possible since they strongly depend on sample preparation conditions. The fitting results are shown in Fig. 6, with a 0.2° mean-square deviation. Thermal conductivities of a number of other thin films are also obtained, all with good fitting between the measured and theoretical data.[13] Results of these measurements verified the validity of the theoretical model developed in this work.

The PA model developed in this work can also be used for a single layer having nonhomogeneous thermal or optical properties. This is done by treating the nonhomogeneous portion with a system of homogeneous plane layers.[5,14] On the other hand, in a multilayer thin film system, not all the layers have to be considered if heat does not penetrate into all the layers. In fact, for thermally thick multilayer samples, numerical overflow can occur in the calculation. This problem can be prevented by discarding all the layers after the first thermally thick layer.

The PA formula developed here is based on the assumption of uniform laser irradiation, however, it also can be used for the case of arbitrary laser energy distribution. This is because the PA signal is independent of the energy distribution of the incident laser beam as long as thermal diffusion in the sample or gas is not beyond the wall of the gas cell.[8,15]

The limitations of the theoretical model developed in this work include that absorption of light in the sample must be treated as exponential, and multiple reflection and interference effects in the sample are neglected. The equations of PA signal are not expected to be valid when multiple reflection and interference occur. In practice, in order to perform PA measurements on samples with weak absorption or with internal reflection and interferences, the surface of the sample can be coated with an absorbing thin film in which the light can be completely absorbed. This treatment is efficient, particularly for transparent samples or samples with complex structures.

IV. CONCLUSION

In this work, a generalized model for the photoacoustic effect is developed. This model can be used for materials with multilayers, all of which might absorb incident radiation, and between which thermal contact resistance can exist. With this model, PA spectroscopy with the unique capability of performing depth-profile analyses can be used to its full potential in the study of multilayer, nonhomogeneous substances. In addition, the composite piston model of the PA effect is derived based on the thermodynamics principles, which clarifies the physical meaning of the action of each piston. The compression process of the thermal piston is confirmed to be isochoric by experimental data, and the compression process of the mechanical piston is found to be polytropic with a factor of $(2-1/\gamma)$. The model developed in this work is verified by measuring thermal conductivity and thermal contact resistance of a number of samples, and good agreements are obtained between the measured data and the available literature values.

[1] A. Rosencwaig and A. Gersho, J. Appl. Phys. **47**, 64 (1976).
[2] F. A. McDonald and G. C. Wetsel, J. Appl. Phys. **49**, 2313 (1978).
[3] N. C. Fernelius, J. Appl. Phys. **51**, 650 (1980).
[4] Y. Fujii, A. Moritani, and J. Nakai, Jpn. J. Appl. Phys. **20**, 361 (1981).
[5] S. D. Campbell and S. S. Yee, IEEE Trans. Biomed. Eng. **26**, 220 (1979).
[6] J. Baumann and R. Tilgner, J. Appl. Phys. **58**, 1982 (1985).
[7] K. D. Cole and W. A. McGahan, Micromechanical Systems, Proceedings of Winter Annual Meeting of the American Society of Mechanical Engineering (ASME, New York, 1992), p. 267.
[8] C. A. Bennett and R. R. Patty, Appl. Opt. **21**, 49 (1982).
[9] F. A. McDonald, Appl. Phys. Lett. **36**, 123 (1980).
[10] P. Korpiun and B. Büchner, Appl. Phys. B: Photophys. Laser Chem. **30**, 121 (1983).
[11] F. P. Incropera and D. P. DeWitt, *Fundamentals of Heat and Mass Transfer* (Wiley, New York, 1990).
[12] M. Okuda and S. Ohkubo, Thin Solid Films **213**, 176 (1992).
[13] X. Wang, H. Hu, and X. Xu, 1999 National Heat Transfer Conference and Publication in the Conference Proceedings (unpublished).
[14] J. Opsal and A. Rosencwaig, J. Appl. Phys. **53**, 4240 (1982).
[15] R. S. Quimby and W. M. Yen, J. Appl. Phys. **51**, 1252 (1980).